# Observation of Accelerated Nucleation in Dense Colloidal Fluids of Hard Sphere Particles

J. L. Harland, S. I. Henderson, S. M. Underwood, and W. van Megen
*Department of Applied Physics, Royal Melbourne Institute of Technology, Melbourne, Victoria 3000, Australia*
(Received 7 July 1995)

Crystallization of a suspension of hard spherical polymer particles is measured by following the evolution of the main Bragg reflection from the close-packed planes. Crystal growth, evident below the melting concentration, is effectively suppressed at higher concentrations due to superlinear rates of crystal addition. We discuss these results in terms of classical nucleation theory. We conclude that superlinear nucleation rates may be a general characteristic of crystallization under constant volume conditions following a deep quench in systems where the crystal phase is of higher density than the fluid.

PACS numbers: 82.70.Dd, 64.70.Dv, 81.10.Fq

Homogeneous nucleation of crystals in an undercooled fluid remains one of the more intriguing aspects of condensed matter. Nucleation is generally considered to occur at a constant rate, possibly preceded by a sublinear transient nucleation or induction phase immediately following the quench [1]. The notion of a constant nucleation rate is, to a large extent, dictated by limited experimental resolution due to the extremely fast crystallization of quenched molecular fluids. Colloidal suspensions, however, present themselves as an experimental model by which we might gain further insight into crystallization kinetics. The mechanical fragility of colloidal crystals and their slow regrowth after shear melting overcome some of the major experimental hurdles encountered in molecular systems. Below the glass transition concentration crystallization has been observed to occur by homogeneous nucleation [2,3]. Growth on container walls or impurities, effects that so often confound nucleation measurements in undercooled molecular fluids [1], appear to be absent. Recent crystallization studies [4,5] on suspensions of hard-sphere-like particles, chosen because they mimic the phase behavior of atomic systems [2,3], indicate that up to about the melting concentration crystallization occurs by a constant nucleation rate accompanied by diffusion limited growth. However, the extent to which nucleation and growth compete at higher particle concentrations, or supersaturations, remains to be explored.

In this Letter we present results of measurements of the growth of the orientationally averaged main Bragg reflection during the crystallization of suspensions of hard colloidal particles at concentrations up to that of the glass transition. Above the melting concentration we find that the nucleation is significantly faster than linear while growth is essentially suppressed. We explain these findings within the framework of classical nucleation theory.

We use suspensions of polymethylmethacrylate particles (radius $a = 200$ nm) made nearly transparent, and therefore suitable for light scattering studies, by closely matching the refractive index of the suspending liquid to that of the particles. A solvated macromolecular layer (approximately 10 nm thick) chemically grafted to the particle surfaces provides steric stability through steeply repulsive interparticle forces. Freezing, melting, and glass transition volume fractions are, as expected for the hard sphere system, identified at $\phi_f = 0.494$, $\phi_m = 0.545$, and $\phi_g \approx 0.58$, respectively [2,3,6]. Crystallization in these suspensions shares features observed in molecular systems such as disilicates and metals [1]. Between $\phi_f$ and $\phi_g$ crystallization occurs by homogeneous nucleation, evidenced by the spontaneous appearance of crystals randomly distributed throughout the sample volume, while for $\phi > \phi_g$ homogeneous nucleation is suppressed but crystal growth occurs on secondary nuclei such as container walls and remnant structures induced by the shear melting process [3].

The main features of the orientationally averaged diffraction pattern consist of a Bragg reflection from the close-packed planes, superimposed on a broad diffuse background associated with the random stacking of these planes [7]. To monitor the evolution of this reflection a volume $V = 0.64$ cm$^3$ of the sample, contained in a cuvette of 1 cm square cross section, was illuminated by the beam of a 3 mW diode laser ($\lambda = 678.7$ nm). The scattered light was collected by a linear diode array camera. The experimental arrangement provided a spatial window, between scattering vectors $q_1$ and $q_2$, of sufficient extent $[(q_2 - q_1)/q_m \approx 0.1]$ and resolution $(\delta q/q_m \approx 0.0005)$ to capture the main Bragg reflection centered at the scattering vector $q_m$.

Each sample was gently tumbled for several hours, to provide a shear melted metastable colloidal fluid, before placing it in the spectrometer. Subsequently, intensity profiles $I(q;t)$ were collected by the camera at preset time intervals to a final time $t_f = 20$ h. The close refractive index match of particles and suspending liquid precluded accurate measurement of the single particle form factor $P(q)$ on dilute suspensions. Therefore, $P(q)$ was estimated from $\alpha P(q) = I(q;0)/S_{\mathrm{PY}}(q)$, where $\alpha$ is a sample dependent contrast factor and $S_{\mathrm{PY}}(q)$ is the Percus-Yevick structure factor for the hard sphere fluid at the same (hard sphere) volume fraction $\phi$ as the sample. Previous work has shown that, for $\phi_f < \phi < \phi_g$ and in

 0031-9007/95/75(19)/3572(4)$06.00 

the vicinity of $q_m$, the static structure factors of metastable colloidal fluids, of particles similar to those used here, are accurately described by the Percus-Yevick result for hard spheres [8]. Division of the intensities by the form factors then gave the net structure factors $S(q;t) = I(q;t)/\alpha P(q)$ of fluid plus crystal. Structure factors $S_c(q;t)$ of the developing crystals were subsequently obtained by subtracting the diffuse intensity scattered by the fluid,

$$S_c(q;t) = S(q;t) - \beta(t) S_{PY}(q) . \quad (1)$$

The scale factor $\beta(t)$ was adjusted so that $S_c(q_1;t) = 0$. The degree of crystallinity $X(t)$ after shear melting of a sample was determined from the area,

$$X(t) = \gamma \int_{\Delta q} S_c(q;t)\, dq , \quad (2)$$

under the main peak. For each sample the integration window $\Delta q$ was selected prior to shear melting to isolate the main Bragg peak. The constant $\gamma$ was chosen so that $X(t_f) = 1$ for the sample closest to the melting concentration. Justification of this procedure is evidenced by the fact that the time variation of the quantity $1 - \beta(t)$ is similar to that of $X(t)$. We also calculated the average linear crystal size,

$$L(t) = 2\pi K / w_q(t) a , \quad (3)$$

where $w_q(t)$ is the width of the peak at half maximum and $K = 1.155$ is the Scherrer constant for a crystal of cubic shape [9]. The number density of (average sized) crystals is then

$$N_c(t) = X(t)/L^3(t) , \quad (4)$$

and, assuming a close-packed structure, the particle volume fraction of the crystal is

$$\phi_c(t) = 0.0130[q_m(t)a]^3 . \quad (5)$$

Results for the degree of crystallinity $X(t)$ and the average linear crystal dimension $L(t)$ are shown in Figs. 1 and 2, respectively, for several suspension volume fractions $\phi$ in the range $0.530 < \phi < 0.575$. Values of $X(t_f) > 1$ seen at the higher concentrations may be associated with a reduction in stacking faults [7]. For the lowest volume fractions ($\phi \lesssim \phi_m$) the data for $L(t)$ suffer from considerable statistical uncertainties, due to poor orientational averaging over the relatively small numbers of crystals in the illuminated region. These data are too inaccurate to specify growth rate exponents with confidence, but one can see, nonetheless, that the initial increase in $X(t)$ is accompanied by a significant increase in $L(t)$. However, as $\phi$ is increased beyond $\phi_m$, the crystal size remains almost constant over the time interval where $X(t)$ shows the largest increase. In addition, the most rapid rate of increase in $X(t)$, which is seen to occur with gradually decreasing growth exponents [from about 4 ($J4$) to 3 ($J6$) then to 2 ($J8$)], is preceded by a slower rate of increase

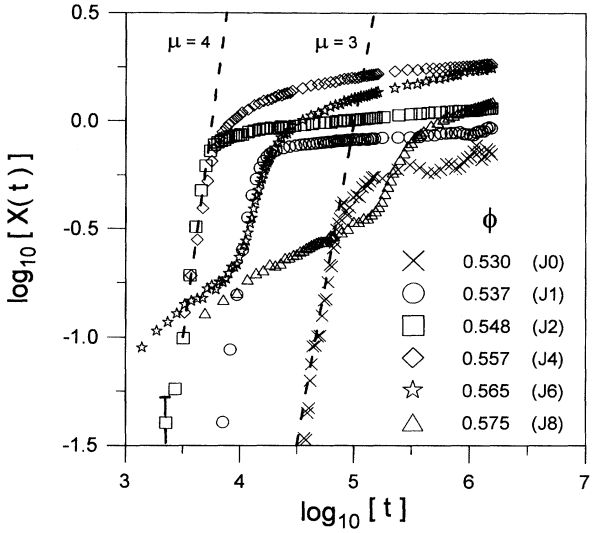


FIG. 1. Degree of crystallinity $X(t)$ [Eq. (2)] versus dimensionless time $t$ expressed in units of $\tau_b = a^2/D_0$, where $D_0$ is the free particle diffusion coefficient. Effective hard sphere volume fractions $\phi$ and our designations are indicated. Power laws $t^\mu$ are shown by dashed lines with indicated exponents $\mu$. Estimates of uncertainties incurred in the measurements and background subtraction are indicated for $X(t) \lesssim 0.1$. These are negligible for $X(t) \gtrsim 0.1$.

that becomes sublinear as the glass transition concentration is approached.

The apparent change in crystallization dynamics that occurs around the melting concentration is seen more explicitly in Fig. 3, where we plot the crystal number densities as functions of time. The most striking feature is that both the fastest rate of crystal addition and the

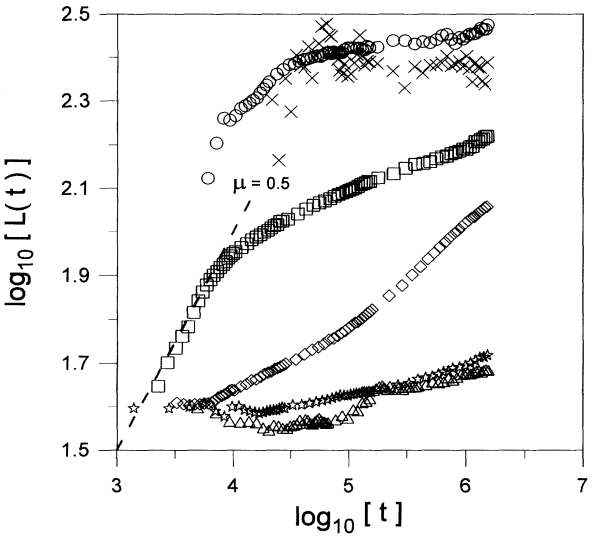


FIG. 2. Average linear crystal dimension $L(t)$ [Eq. (3)] versus dimensionless time. Symbols are as indicated in Fig. 1.

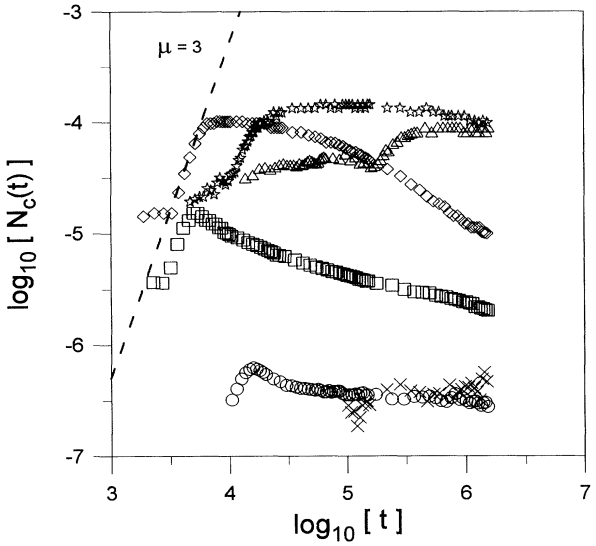


FIG. 3. Number density of crystals $N_c(t)$ [Eq. (4)] versus dimensionless time. Symbols are as indicated in Fig. 1.

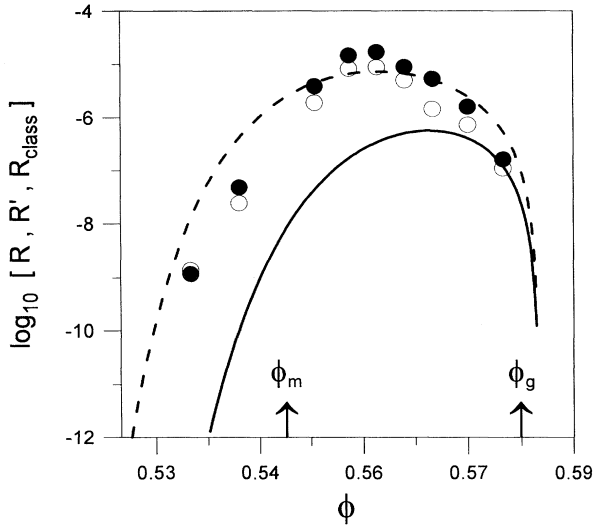


FIG. 4. Maximum and average nucleation rate densities, $R$ (filled circles) and $R'$ (open circles), versus volume fraction. Theoretical results [Eq. (6)] are shown for $\gamma = 0.5$ (dashed curve) and $\gamma = 0.65$ (solid curve).

maximum number of crystals increase sharply (by more than 2 orders of magnitude) as the melting concentration is traversed. For $\phi \gtrsim \phi_m$ the early time dependence of $N_c(t)$ reflects that of $X(t)$, a slow increase initially which then accelerates to $N_c(t) \sim t^3$.

The fast increase in $X(t)$ (Fig. 1) crosses over to a region where it is either almost constant ($\phi \lesssim \phi_m$) or increases at a much slower rate ($\phi \gtrsim \phi_m$). The accompanying slow increase in $L(t)$ (Fig. 2) and slow decrease in $N_c(t)$ (Fig. 3) suggest coarsening, the growth of larger crystals at the expense of the smaller ones. Since the largest growth exponents $\nu$ for the average linear crystal dimension (Fig. 2) attained at long times range from about 0.005 to 0.2, it appears that the classical coarsening process of crystals in contact (for which $\nu = 0.5$) [10] has not been reached during the period of observation.

Figure 4 shows the maximum nucleation rate densities $R$ calculated from the maximum slopes of $N_c(t)$ vs $t$ (Fig. 3), and average nucleation rate densities $R'$ obtained from the maxima in $N_c$. Coincidence of $R$ and $R'$ indicates that, for $\phi \gtrsim \phi_m$, nucleation occurs by an accelerated "burst" of nuclei. The sudden emergence of large numbers of nuclei in the sample, with an average spacing of only about 30 particle diameters, apparently restricts crystal growth of macroscopic significance (Fig. 2). At the lowest concentrations, where significant early growth is observed, the results of Fig. 4 do not preclude the possibility of a constant rate of crystal addition.

For hard spheres the classical nucleation rate density can be expressed as [11,12]

$$R_{\text{class}} = A\phi^{5/3} D \exp\{-4\pi^3\gamma^3/27\phi^2\Delta\mu^2\}, \quad (6)$$

where $\gamma$ [in units of $(2a)^2/kT$] is the surface tension of the crystal-fluid interface, $\Delta\mu(\phi)$ (in units of $kT$) is the difference in chemical potential between crystal and fluid phases, and the dynamical factor $A$ is expected to be of order unity. Differences between the present and previous [11,12] evaluations of $R_{\text{class}}$ are that we use the Carnahan-Starling equation of state for the hard sphere fluid [13] and for the long-time (dimensionless) self-diffusivity the expression $D = (1 - \phi/\phi_g)^{2.58}$. The latter describes the slow structural relaxation rates measured for concentrated metastable colloidal fluids of hard spheres [14]. We consider this to be more appropriate than a formula fitted to diffusion coefficients measured on equilibrium fluids below $\phi_f$. In Fig. 4 we show $R_{\text{class}}$ for two values of $\gamma$ (0.50 and 0.65) that span current estimates for the surface tension of the crystal-fluid interface of hard spheres [12]. The agreement between the experimental and predicted results is obtained with $A = 100$. This value for the dynamical factor may be compared with $A = O(10^{10})$ typically found for molecular systems [1].

In Fig. 5 we show the crystal volume fractions $\phi_c(t)$ calculated from the Bragg peak positions [Eq. (5)]. The first identifiable crystals have a significantly higher volume fraction than the average volume fraction of the sample, i.e., the initial volume fraction of the metastable fluid (listed in Fig. 1). However, we infer, with the aid of the equations of state of the hard sphere crystal [15] and the metastable fluid [13], that these crystals are in approximate mechanical equilibrium with the fluid. Furthermore, as the coincidence of the time intervals of the steepest reduction in $\phi_c(t)$ and the steepest increase in $X(t)$ suggests, this pressure balance is maintained, at least in part, during the conversion of colloidal fluid into the more compact crystal. Thus, when a colloidal fluid is

quenched, nucleation results in a reduction in the concentration and a concommitant increase in the particle diffusivity of the remaining fluid. If the concentration of the quenched fluid exceeds that at which the nucleation rate has a maximum (i.e., $\phi_m \lesssim \phi < \phi_g$ in Fig. 4), then the increase in diffusivity following any nucleation is greater than the increase in the nucleation barrier [the exponent in Eq. (6)]: Nucleation accelerates as a consequence (as seen in Fig. 3).

Initial sublinear rates of conversion from fluid to crystal and crystal addition, evident only at the highest concentrations in (Figs. 1 and 3), could also be present at lower concentrations but hidden by poor resolution. In molecular fluids sublinear transients are attributed to the thermodynamic requirement of an increase of the average cluster size in the wake of a temperature quench [1]. In the present experiments the sublinear transients may be a consequence of the competing slow dissipation of asymmetric, and therefore thermodynamically unstable, structures that are induced by the shear melting [3]; i.e., the clusters that survive the density quench of a colloidal fluid have the wrong shape rather than the wrong size.

Finally, one sees in Fig. 5 that for $\phi < \phi_m$ proximity to equilibrium at the end of the observation period is indicated by the approach of the crystal volume fraction to the melting value, $\phi_c(t \to t_f) \approx \phi_m$. However, the increasing difference $\phi_c(t \to t_f) - \phi$ between the final measured volume fraction of the crystal and the total volume fraction of the sample indicates that the approach to the equilibrium crystal state (i.e., $\phi_c = \phi$) slows considerably with increasing concentration.

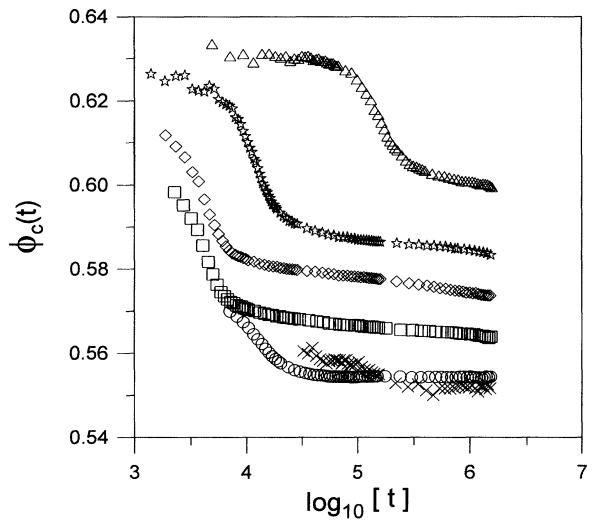


FIG. 5. Volume fraction of the crystal phase, calculated from the Bragg peak positions [Eq. (5)], versus dimensionless time. Symbols are as indicated in Fig. 1.

We conclude that accelerated nucleation, observed here in suspensions of hard spherical particles quenched to a concentration higher than that of the nucleation rate maximum, is a general feature of crystallization occurring in a system of fixed volume when, at mechanical equilibrium, the density of the crystal phase exceeds that of the fluid phase. We speculate that molecular systems, even when the density difference between crystal and fluid is negligible and the pressure instead of the volume is fixed, when quenched to the low temperature side of the nucleation rate maximum may also experience accelerated nucleation due to the reduction of the viscosity of the embedding fluid that results from release of latent heat. However, any underlying accelerated nucleation will necessarily be hidden if a constant rate of nucleation is assumed.

We thank Bruce Ackerson, Peter Harrowell, and Jürgen Müller for many valuable discussions and Phil Francis for his technical assistance. This work was supported by the Australian Research Council.

[1] K. F. Kelton, Solid State Phys. **45**, 75 (1991).
[2] P. N. Pusey and W. van Megen, Nature (London) **320**, 340 (1986).
[3] W. van Megen and S. M. Underwood, Nature (London) **362**, 616 (1993).
[4] B. J. Ackerson and K. Schätzel, Phys. Rev. Lett. **68**, 337 (1992); K. Schätzel and B. J. Ackerson, Phys. Rev. E **48**, 3766 (1994).
[5] Y. He, B. J. Ackerson, W. van Megen, S. M. Underwood, and K. Schätzel (to be published).
[6] S. M. Underwood, J. R. Taylor, and W. van Megen, Langmuir **10**, 3550 (1994).
[7] P. N. Pusey, W. van Megen, P. Bartlett, B. J. Ackerson, J. G. Rarity, and S. M. Underwood, Phys. Rev. Lett. **63**, 2753 (1989).
[8] W. van Megen and P. N. Pusey, Phys. Rev. A **43**, 5429 (1991).
[9] R. W. James, in *The Optical Principles of the Diffraction of X-Rays,* edited by L. Bragg (Cornell Univ. Press, New York, 1965).
[10] I. Lifshitz and V. Solyozov, J. Phys. Chem. Solids **19**, 35 (1961); S. Allan and J. Cahn, Acta Metall. **24**, 425 (1979).
[11] W. B. Russel, Phase Transit. **21**, 127 (1990).
[12] J. S. van Duijneveldt and H. N. W. Lekkerkerker, in *Science and Technology of Crystal Growth,* edited by J. P. van Erde and O. S. L. Bruinsma (Kluwer Academic, Dordrecht, 1995).
[13] N. F. Carnahan and K. E. Starling, J. Chem. Phys. **51**, 635 (1969).
[14] W. van Megen and S. M. Underwood, Phys. Rev. E **49**, 4206 (1994).
[15] K. R. Hall, J. Chem. Phys. **57**, 2252 (1972).